UNIVERSIDADE DE SÃO PAULO

INSTITUTO DE FÍSICA
CAIXA POSTAL 20516
01498 - SÃO PAULO - SP
BRASIL

publicações

IFUSP/P-477

THE ROLE OF PERIPHERAL PARTIAL WAVES IN THE ANOMALOUS LARGE ANGLE SCATTERING OF n-α NUCLEI

by

A.N. Aleixo, L.F. Canto and P. Carrilho
Instituto de Física, Universidade Federal do Rio de Janeiro, 21910 Rio de Janeiro, RJ, Brazil

and

M.S. Hussein
Instituto de Física, Universidade de São Paulo

Julho/1984

THE ROLE OF PERIPHERAL PARTIAL WAVES IN THE ANOMALOUS LARGE ANGLE SCATTERING OF n-α NUCLEI*

A.N. Aleixo, L.F. Canto and P. Carrilho
Instituto de Física, Universidade Federal do Rio de Janeiro,
21910 Rio de Janeiro, R.J., Brazil

and

M.S. Hussein
Instituto de Física, Universidade de São Paulo,
C.P. 20516, São Paulo, S.P., Brazil

ABSTRACT

Properties of the elastic excitation function at 180^{o} produced by deviations from the usual strong absorption S-matrix are studied. We consider deviations $\tilde{S}$ with the shape of windows in ℓ-space, centered around a value $\bar{\ell}$ corresponding to a peripheral collision and concentrate our analysis in the interference of the partial waves neighbouring $\bar{\ell}$. The conditions for constructive and destructive interference and the effect of odd-even staggering factors are investigated, in the presence and in the absence of Coulomb and nuclear refraction. The consequences of such interference on the anomalous behaviour of the 180^{o} excitation function for the elastic scattering of some n-α nuclei are discussed, in connection with results of other works.

*Supported in part by FINEP, CNPq and FAPESP.

July/1984

1. INTRODUCTION

The anomalous behaviour of the cross-sections for collisions between n-α nuclei (e.g. ^{12}C, ^{16}O, ^{20}Ne, ^{24}Mg, ^{28}Si, ^{32}S, etc.) has been intensively studied in the last seven years[1]. Contrasting with the typical optical model like pattern observed in most Heavy Ion collisions the elastic cross-section for collisions of these nuclei is strongly enhanced at large angles and the 180^{o} excitation function is dominated by pronounced oscillations. Similar abnormal cross sections are also observed in inelastic and α-transfer channels.

Although the dynamical origin of such anomalies has not yet been satisfactorily established, it has been shown[2,3] that the main tendencies of the large angle elastic scattering data can frequently be reproduced by the addition of two anomalous contributions $\tilde{S}(\ell,E)$ and $\tilde{S}'(\ell,E)$ to the normal strong absorption S-matrix[2]. These contributions have the shape of windows in ℓ-space, representing peripheral collisions, and $\tilde{S}'(\ell,E)$ contains an odd-even staggering factor $(-)^{\ell}$ as that appearing in elastic transfer processes. This factor affects drastically the contribution of $\tilde{S}'$ to the cross-section. While the relevant partial waves usually interfere destructively, producing cancellations, the factor $(-)^{\ell}$ changes the relative phases between consecutive ℓ-values and may lead to constructive interference.

In the present paper we study in detail the interference between the partial waves describing peripheral collisions which contribute to the elastic cross-section through the anomalous terms $\tilde{S}(\ell,E)$ and $\tilde{S}'(\ell,E)$. We discuss also how the results of this study affect the conclusions of other papers[2,3,4,5] in which the anomalous elastic scattering of n-α nuclei is attributed to peripheral processes. In Section 2

we stablish our notation and introduce some useful analytical expressions based on the Poisson series. In section 3 we study the influence of the details of $\bar{S}(\ell,E)$ and $\tilde{S}(\ell,E)$ on the interference of the partial waves. In section 4 we show how cancellation or enhancement effects resulting from the interference of peripheral waves may affect the trends of the 180° excitation function. Finally a summary of the main conclusions of the present work is presented in section 5.

Throughout this paper we will consider exclusively 180° excitation functions. This choice is justified by the facts that the information it contains are much richer than those contained in angular distributions and that analytical expressions become much simpler at 180°.

2. BASIC NOTIONS, ANALYTICAL FORMULAE

We write the partial-wave projected S-matrix as

$$S(\ell,E) = e^{i2\sigma_\ell}\left(\bar{S}^N(\ell,E) + \tilde{S}^N(\ell,E)\right) \qquad (2.1)$$

where $\bar{S}^N$ is the usual "strong absorption profile"[2] corresponding to strongly absorbing optical potentials and $\tilde{S}^N(\ell,E)$ is an anomalous contribution associated with peripheral processes. Assuming that the 180° excitation function is not affected by $\bar{S}(\ell,E)$ we may write

$$\frac{d\sigma}{d\Omega}(180^{\circ},E) = \left|\frac{1}{ik}\sum_{\ell=0}^{\infty}(\ell+1/2)(-)^{\ell}\,\tilde{S}^N(\ell,E)\,e^{2i\sigma_\ell}\right|^2 \qquad (2.2)$$

In the above equation σ_ℓ are Coulomb phase shifts, k is the relative wave number and the factor $(-)^{\ell}$ corresponds to the Legendre Polynomials at 180°. It is convenient to write $\tilde{S}^N(\ell,E)$ as

$$\tilde{S}^N(\ell,E) = d(E)\,\omega(\ell-\tilde{\ell}) \qquad (2.3)$$

where d(E) is an overall energy dependent strength and $\omega(\ell-\bar{\ell})$ represents a window in ℓ-space centered at $\ell=\bar{\ell}$ with the normalization $\omega(0)=1$. The quantity $\tilde{\ell}$ characterizes the peripheral nature of the process and is given by the semi-classical relation[2]

$$\tilde{\ell}+1/2 \equiv \tilde{\Lambda} = \tilde{R}\sqrt{\frac{2\mu}{\hbar^2}}\sqrt{E-E_B} \qquad (2.4)$$

In order to study the interference between the partial waves neighbouring $\bar{\ell}$ it is convenient to put eq. (2.2) into the form

$$\frac{d\sigma}{d\Omega}(180^{\circ},E) = g(E)\cdot|d(E)|^2\cdot a(E) \qquad (2.5)$$

with

$$g(E) \equiv \left(\frac{\tilde{\Lambda}}{k}\right)^2 = \tilde{R}^2\left(1-\frac{E_B}{E}\right) \qquad (2.6)$$

$$a(E) = \left|\sum_{\ell=0}^{\infty}\frac{\ell+1/2}{\tilde{\Lambda}}\,e^{2i\sigma_\ell}(-)^{\ell}\,\omega(\ell-\tilde{\ell})\right|^2 \qquad (2.7)$$

g(E) is a purely geometrical factor which tends to the limit $\tilde{R}^2$ as the scattering energy increases. The interference factor a(E), on the other hand expresses the interference aspects of the

partial waves. In the simple case that $\omega(\ell,\tilde{\ell}) = \delta(\ell,\tilde{\ell})$ one gets $a(E) = 1$. If ω has a finite width $a(E)$ will have contributions from other partial waves and the net result may be cancellation or enhancement. In the former case $a(E) < 1$ and in the latter $a(E) > 1$.

In our study of $a(E)$ we will use two different shapes for $\omega(\ell,\tilde{\ell})$. A gaussian shape (GP)

$$\omega(\ell-\tilde{\ell}) = \exp[-(\ell-\tilde{\ell})^2/2\sigma^2] \tag{2.8}$$

and the derivative of a real Ericson function[6] (DEP)

$$\omega(\ell-\tilde{\ell}) = 2\left[1+\cosh\left(\frac{\lambda-\tilde{\Lambda}}{\tilde{\Delta}}\right)\right]^{-1} \tag{2.9}$$

As we will see below, these shapes have the advantage of leading to analytical expressions for $a(E)$.

To calculate $a(E)$ we will follow Frahn[7]. As a starting point we write the Poisson formula for $\tilde{f}(\theta=180^\circ)$

$$\tilde{f}(180^\circ) = -\frac{i}{k}\sum_{m=-\infty}^{\infty} e^{i\pi(m+1/2)} \cdot \int_0^\infty d\lambda\, \lambda\, \tilde{S}^N(\lambda)\exp[2i(2\sigma(\lambda)+2\pi(m+1/2)\lambda)] \tag{2.10}$$

where $\lambda = \ell + \frac{1}{2}$ and $\tilde{S}^N(\lambda)$ and $\sigma(\lambda)$ are analytic continuations of $\tilde{S}^N(\ell,E)$ and σ_ℓ. If the Coulomb phase-shifts can be expanded linearly around $\tilde{\Lambda}$,

$$2\sigma(\lambda) \cong \tilde{\theta}_R(\lambda-\tilde{\Lambda}) + 2\sigma(\tilde{\Lambda}) \; ; \; \tilde{\theta}_R = \theta_R(\tilde{\Lambda}) = 2\tan^{-1}\left(\frac{\eta}{\tilde{\Lambda}}\right) \tag{2.11}$$

in the whole region of λ-space where $\tilde{S}^N$ is relevant, Frahn shows[7] that

$$f(180^\circ) \cong -i\frac{\tilde{\Lambda}}{k} e^{2i\sigma(\tilde{\Lambda})}\, d(E)\, \mathcal{N} \cdot \sum_{m=-\infty}^{\infty} e^{i\pi(2m+1)\tilde{\ell}}\, H[\tilde{\theta}_R+(2m+1)\pi] \tag{2.12}$$

with

$$H(z) = \int_{-\infty}^{\infty} d\lambda\, \frac{\omega(\lambda-\tilde{\Lambda})}{\mathcal{N}}\, e^{i(\lambda-\tilde{\Lambda})z} \tag{2.13}$$

and

$$\mathcal{N} = \int_{-\infty}^{\infty} \omega(\lambda-\tilde{\Lambda})\, d\lambda \tag{2.14}$$

The interference factor takes the form

$$a(E) = \mathcal{N}^2 \left| \sum_{m=-\infty}^{\infty} e^{i\pi(2m+1)\tilde{\ell}}\, H[\tilde{\theta}_R+(2m+1)\pi] \right|^2 \tag{2.15}$$

For the DEP (eq. (2.9)) one finds[7]

$$H(z) = \frac{\pi\tilde{\Delta}z}{\sinh(\pi\tilde{\Delta}z)}\, e^{i\tilde{\alpha}\tilde{\Delta}z} \tag{2.16}$$

and

$$\mathcal{N} = 4\tilde{\Delta} \tag{2.17}$$

For the GP of eq. (2.8) it can be easily shown that

$$H(z) = \exp[-\sigma^2 z^2/2] \tag{2.18}$$

and

$$\mathcal{N} = \sigma\sqrt{2\pi} \tag{2.19}$$

We are also interested in the odd-even staggering* with these parametrization, i.e.

$$\omega'(\lambda-\tilde{\Lambda}) = e^{i\beta\pi\lambda}\,\omega(\lambda-\tilde{\Lambda}) \tag{2.20}$$

with $\beta = -1$**. In these cases it is straightforward to show that the normalization $\mathcal{N}$ is unchanged and the function $H'(z)$ can be expressed in terms of $H(z)$ through the relation

$$H'(z) = e^{i\beta\pi\tilde{\Lambda}}\,H(z+\beta\pi) \tag{2.21}$$

The above relation holds not only for odd-even staggering but also in any case where the difference of phase between $\omega'(\lambda-\tilde{\Lambda})$ and $\omega(\lambda-\tilde{\Lambda})$ depends linearly on λ.

3. STUDY OF THE INTERFERENCE FACTOR

In this section we will study the interference factors $a(E)$ and $a'(E)$ in different situations. We will consider the DEP and GP shapes of $\omega(\lambda-\tilde{\Lambda})$, the effects of refraction on $a(E)$ and $a'(E)$ and also the effects of asymmetry of $\omega(\lambda-\tilde{\Lambda})$ with respect to $\tilde{\Lambda}$.

*We will adopt the notation that primes are always associated with odd-even staggering.

**Clearly a $\beta = 1$ is also possible. However we choose the negative sign so that even-odd staggering may be viewed as a form of nuclear refraction (negative).

a) No refraction limit

Let us consider first the limiting, hypothetical, case where both Coulomb and nuclear phases are neglected ($\sigma_\ell = \delta_\ell^N = 0$). In this case $\tilde{\theta}_R = 0$ and no expansion of σ_ℓ is needed. The Poisson series is strongly dominated by the terms $m = -1$ and $m = 0$ (except when σ or $\tilde{\Lambda} \ll 1$) and we get

$$a(E) = C\cos^2(\pi\tilde{\ell}(E)) \tag{2.22}$$

$$a'(E) = C' \tag{2.23}$$

where C and C' are the energy independent quantities

$$C = \begin{cases} (4\pi\tilde{\Lambda})^2 e^{-2\pi^2\tilde{\Delta}} & , \text{ for de DEP} \\ 8\pi\sigma^2\, e^{-\sigma^2\pi^2} & , \text{ for de GP} \end{cases} \tag{2.24}$$

and

$$C' = \begin{cases} 16\,\tilde{\Delta}^2 & , \text{ for the DEP} \\ 2\pi\sigma^2 & , \text{ for the GP} \end{cases} \tag{2.25}$$

For the purpose of comparing the DEP and the GP it is convenient to express the parameters $\tilde{\Delta}$ and σ in terms of the half-width $\tilde{\Gamma}$

$$\sigma = \tilde{\Gamma}/1.18 \tag{2.26}$$

$$\tilde{\Delta} = \tilde{\Gamma}/1.76 \tag{2.27}$$

The constant C' gives an energy independent upper limit for the odd-even staggering interference factor $a'_{(E)}$ in the presence of refraction. In the no-refraction case the contributions from all partial waves are aligned along the positive direction of the real-axis. The presence of refraction introduces energy dependent relative phases among the partial wave and the coherence is weakened.

On the other hand, the no-refraction limit in the absence of odd-even staggering gives the strongest cancellation possible. The interference factor shows strong oscillations resulting from the terms $m = -1$ and $m = 0$, which have the same amplitude, with the "natural" period

$$P_o(E) = \left(\frac{d\tilde{\ell}(E)}{dE}\right)^{-1} \tag{2.28}$$

determined by the condition $\delta\tilde{\ell}(E) = 1$. Although the period of oscillation depends on E, the maxima of $a(E)$ are tangent to the energy independ quantity C.

A comparison between the interference factors resulting from the two parametrizations with the same half-width $\tilde{\Gamma}$ indicates that the DEP produces stronger enhancement in C' while nothing can be said about cancellation in $a(E)$ as the comparison depends on $\tilde{\Gamma}$.

b) Pure Coulomb refraction

To perform calculations with Coulomb refraction it is necessary to specify a system in order that $\tilde{\ell}(E)$ and σ_ℓ can be evaluated. We choose $^{16}O + ^{28}Si$ for which there is a lot of information available. It should be mentioned,

however, that the main features of $a(E)$ and $a'(E)$ are qualitatively the same for other n-α systems. For $^{16}O + ^{28}Si$ $\tilde{\Lambda}$ is given by eq. (2.4) with

$$\tilde{R} = 7.36 \text{ fm} \tag{2.29a}$$

$$E_B = 17.8 \text{ Mev} \tag{2.29b}$$

If the width is not too small and the energy not too high (too low), the factor $a(E)$ ($a'(E)$) is dominated by $m = -1$ (0) in the Poisson series. Keeping only these leading terms we obtain

$$a(E) = \left[4\pi(\tilde{\theta}_\ell - \pi)\tilde{\Delta}^2 / \sinh(\pi\tilde{\Delta}(\theta_\ell - \pi))\right]^2 \tag{2.30}$$

$$a'(E) = \left[4\pi\tilde{\theta}_\ell\tilde{\Delta}^2 / \sinh(\pi\tilde{\Delta}\theta_\ell)\right]^2 \tag{2.31}$$

for the DEP, and

$$a(E) = 2\pi\sigma^2 \exp\left[-\sigma^2(\tilde{\theta}_\ell - \pi)^2\right] \tag{2.32}$$

$$a'(E) = 2\pi\sigma^2 \exp\left[-\sigma^2\tilde{\theta}_\ell^2\right] \tag{2.33}$$

One should keep in mind though that these are approximate expressions based on the condition $\tilde{\Gamma} \ll \tilde{\Lambda}$ and on a linear expansion of the $\sigma_{(\lambda)}$ around $\tilde{\Lambda}$, which may become inappropriate as $E \to E_B$, in which case $\tilde{\Lambda} \to 0$.

In figs. 1 and 2 we show $a(E)$ and $a'(E)$ in the cases of DEP (eq. (2.9)) and GP (eq. (2.8)), respectively. Interference factors obtained by the numerical summation of eq. (2.7) (full lines) and by the approximate expressions (2.30)-(2.33) (crosses) are given for $\tilde{\Gamma} = 1, 2$ and 3. The no-refraction limits c and c' are also indicated in each case. Firstly it should be noticed that the approximate expressions (2.30)-(2.33) give the interference factors with very good accuracy. The shortcoming of missing the large energies oscillations for $\tilde{\Gamma} = 1$ can be easily eliminated by the inclusion of the $m = 0$ term in the Poisson series. Besides, the figures show some interesting features of a and a'.

- The interference factors converge to the no-refraction limits as the energy increases. This is a direct consequence of the fact that $\tilde{\theta}_R$,

$$\tilde{\theta}_R = 2\tan^{-1}\left(\frac{\eta}{\tilde{\Lambda}}\right) = 2\tan^{-1}\left[\frac{11.0}{\sqrt{E(E-E_B)}}\right] \qquad (2.34)$$

goes to zero as $E \to \infty$, and the non-Coulomb-refraction limit is apporached.

- The view that $a(E)$ is dominated by cancellation and that $a'(E)$ by enhancement is not correct. The tendency of the interference factor changes with energy. In fig. (1b), for example, $a(E) < 1$ for $E < 31$ MeV and $a(E) > 1$ for $E < 19$ MeV.

- The factor $a(E)$ intercepts $a'(E)$ at $E_0 = 23.0$ MeV, both for DEP and GP, for any $\tilde{\Gamma}$. E_0 is given by the condition (see eqs. (2.30)-(2.33)) $\tilde{\theta}_R = \pi/4$, or $\tilde{\Lambda}_{(E)} = \eta_{(E)}$. This means that the introduction of an odd-even staggering factor in $\omega(\lambda-\tilde{\Lambda})$ enhances the cancellation at energies below 23 MeV.

We have also investigated the mecanism through which strong cancellation may occur in $a(E)$. For this purpose we introduce the quantity

$$\alpha^{(o-\ell)}_{(E)} \equiv \left| \sum_{\ell'=0}^{\ell'=\ell} \frac{(\ell'+1/2)}{\tilde{\Lambda}} e^{2i\sigma_{\ell'}} \omega(\ell'-\tilde{\ell}) \right|^2 \qquad (2.35)$$

and similarly $\alpha'^{(o-\ell)}_{(E)}$, which are represented in fig. 3 for the DEP at 35 MeV with $\tilde{\Gamma} = 2$. It is shown that the cancellation is an overall property of the partial waves around $\tilde{\ell}$. A naïve interpretation that such cancellation occurs among consecutive partial waves for which the Legendre polynomial gives opposite signs is clearly wrong. If this were the case $\alpha^{(o-\ell)}_{(E)}$ would alternate from large to small values, contradicting fig. 3.

c) <u>Coulomb plus nuclear refraction</u>

Let us consider the simple case where

$$\omega(\lambda-\tilde{\lambda}) = e^{i\tilde{\theta}_N\lambda} \, |\omega(\lambda-\tilde{\lambda})| \qquad (2.36)$$

with $|\omega(\lambda-\tilde{\lambda})|$ given by the DEP or the GP. This is exactly the linear dependence of eq. (2.20) with $\tilde{\theta}_N = \beta\pi$ giving a nuclear deflection. Analytical expressions for $a(E)$ and $a'(E)$ are then trivially derived and the results are those of eqs. (2.30)-(2.33) with the replacement of $\tilde{\theta}_R$ by θ;

$$\theta = \tilde{\theta}_R + \tilde{\theta}_N \qquad (2.37)$$

In fig. 4 we show exact values of $a(E)$ and $a'(E)$

obtained with the DEP with $\tilde{\Gamma} = 2$. Results for the GP or for other $\tilde{\Gamma}$ are qualitatively similar. The interference factors were calculated for $\tilde{\theta}_N = 0, -0.25\pi, -0.5\pi, -0.75\pi$ and $-\pi$. An interesting point to be noticed is that the inclusion of nuclear deflection shifts the no-refraction limit to finite energies. In pure Coulomb refraction the condition $\theta_R = 0$ is fulfilled as $E \to \infty$. In the present case, however the no-refraction condition becomes $\theta = 0$, or

$$\tilde{\theta}_R = 2 \tan^{-1}\left[\frac{11.0}{\sqrt{E_{NR}(E_{NR} - 17.8)}}\right] = -\tilde{\theta}_N \qquad (2.38)$$

The condition above is an equation for E. For example the solution for $\tilde{\theta}_N = -0.5\pi$, is $E_{NR} = 23.0$ MeV, which is in perfect agreement with fig. 4C.

A second point of interest is in connection with the footnotes in p. 7. The factor $a'(E)$ corresponds to $a(E)$ in the presence of the nuclear deflection function $\tilde{\theta}_N = -\pi$. The sequence of figs. 4a),b),c),d), and e) show how the interference factors a and a' change into one another as $\tilde{\theta}_N$ varies continuously from 0 to $-\pi$.

In all cases, $a(E)$ and $a'(E)$ are contained within the two corresponding no-refraction limits (except for the localized $m = 0$, $m = -1$ interference oscillations). It is interesting to remark that these limits correspond to the conditions for obtaining forward (in $a(E)$) and backward (in $a'(E)$ glory scattering. Qualitatively speaking, forward (backward) glory implies refractive enhancement at forward (backward) angles and a corresponding damping at backward (forward) angles. These features are clearly exhibited in Fig. 4.

d) Effects of asymmetry in $\omega(\lambda - \tilde{\Lambda})$

So far, we have considered symmetrical shapes for the ℓ-windows. This is clearly a simplifying assumption, which does not generally correspond to anomalous S-matrix deviations associated with specific physical processes. In this Section, we study the interference factors that result from asymmetric shapes. For simplicity we will restrict the discussion to the case

$$\omega = \exp\left[-(\lambda - \tilde{\Lambda})^2 / 2\sigma_1^2\right] \qquad (2.39)$$

$$\omega = \exp\left[-(\lambda - \tilde{\Lambda})^2 / 2\sigma_2^2\right] \qquad (2.40)$$

The above choice of the shape function have the advantage of leading to easily derivable analytical expressions. It should be mentioned however that we have performed numerical calculations with other asymmetric shape functions and the results were qualitatively similar. Also for the sake of simplicity we will neglect nuclear phase shifts.

In fig. 5 we show $a(E)$ for the parametrization of eq. (2.40) with the half widths $\tilde{\Gamma}_1$ and $\tilde{\Gamma}_2$ taking the values 1.5 and 2 and also the results with $\tilde{\Gamma}_1$ and $\tilde{\Gamma}_2$ interchanged. For comparison the interference factors for the symmetrical GP with $\tilde{\Gamma} = 1.5$ and 2 are also shown. It is interesting to note that the asymmetry leads to oscillation with the "natural" period of eq. (2.28). The average value of $a(E)$ decreases with energy more slowly than those for the symmetric parametrizations. For energies above ~ 32 MeV the interference factor for the $\tilde{\Gamma} = 1.5$ GP is exceeded, showing that the asymmetry attenuates

the cancellation. The effects of interchanging $\tilde{\Gamma}_1$ and $\tilde{\Gamma}_2$ are not relevant. Results along the same lines for a'(E) are presented in fig. 6. In this case the asymmetry does not introduce any significant change. The interference factor lies between those for the symmetric parametrizations and it has the same trend.

The main features of a(E) and a'(E) for the asymmetric shape functions of eq. (2.40) can be understood on the basis of eq. (2.15). In this case we get

$$\mathcal{N} = \sqrt{\frac{\pi}{2}}\,(\sigma_1 + \sigma_2) \tag{2.41}$$

and

$$H(z) = H_1(z) - i\,H_2(z) \tag{2.42}$$

with

$$H_1(z) = \frac{\sqrt{\pi/2}}{\mathcal{N}}\left(\sigma_1 e^{-x_1^2} + \sigma_2 e^{-x_2^2}\right) \tag{2.43}$$

and

$$H_2(z) = \frac{2}{\mathcal{N} z}\left[x_1 D(x_1) - x_2 D(x_2)\right] \tag{2.44}$$

were $x_{1,2} \equiv z\sigma_{1,2}/\sqrt{2}$ and $D(x)$,

$$D(x) = e^{-x^2}\int_0^x e^{t^2}\,dt \tag{2.45}$$

is the Dawson function[8]. The term $H_1(z)$ corresponds simply to an average of the H functions for the two symmetric

distributions with weights σ_1 and σ_2. The term $H_2(z)$, on the other hand, is responsible for the peculiarities of a(E) for the asymmetric parametrization. The fact that the Dawson function varies slowly with x, it has a maximum at x=1 and for large (> 5) x goes to zero as

$$D(x) \xrightarrow[x\to 0]{} \frac{1}{2x}\left(1 + \frac{1}{2x^2} + \cdots\right) , \tag{2.46}$$

has two consequences. The first is that it is necessary to consider a few m values in the Poisson series for a(E) (eq. (2.15)). This point is shown in fig. 7, where the exact a(E) and a'(E) values are compared to those obtained with the use of eqs. (2.41)-(2.44) in eq. (2.15), considering only the dominant m = -1 term. Although it reproduces very well a'(E) and also the average behaviour of a(E), it misses the high energy oscillations. We could however reproduce these oscillations with good accuracy by including the m = 0 and m = -2 terms in eq. (2.15). The second consequence is that H(z) in eq. (2.42) is completely dominated by $H_2(z)$ for very broad asymmetric shapes (both $\tilde{\Gamma}_1$ and $\tilde{\Gamma} \geq 3$). In such a case a(E) becomes several orders of magnitude larger than the interference factors associated with the symmetrical GP with half-widths $\tilde{\Gamma}_1$ and $\tilde{\Gamma}_2$.

3. EFFECTS OF THE INTERFERENCE FACTOR ON THE 180° EXCITATION FUNCTION

In this Section we use several of the conclusions reached above to discuss information about the anomalous

deviations which can be extracted "directly" from the experimental $180^{o} \pm 5^{o}$ excitation function. As was done in the previous section, our discussion is centered on the $^{16}O + ^{28}Si$ elastic scattering system. We employ the DEP for definiteness. In Fig. 8 we summarize our findings concerning the connection between the strength $d(E)$ and the width $\tilde{\Gamma}$ compatibles with the data for different values of the anomalous piece of the nuclear deflection function $\tilde{\theta}_N$. These curves were constructed by fixing $\frac{\sigma}{\sigma_{Ruth}}(180^{o})$ at $E_{CM} = 35$ MeV to be $\sim 10^{-2}$, in accordance with the data, and using Eq. (2.5), namely

$$a(E)\,|d(E)|^{2} = 10^{-2}\,\sigma_{Ruth.}(180^{o})/g(E) \qquad (2.47)$$

which supplies $d(E)$ vs. $\tilde{\Gamma}$, the width associated with $\omega(\ell-\tilde{\ell})$ and consequently $a(E)$ (see Eq. (2.7)).

Since the unitarity condition of the S-matrix imposes the constraint

$$d(E) \leq 1 \qquad (2.48)$$

the maximum values of $\tilde{\Gamma}$, $\tilde{\Gamma}_{max}$, compatible with the constraint are indicated by the intersection of these curves with the dashed lines ($d(E) = 1$). We exhibit the dependence of $\tilde{\Gamma}_{max}$ on $\tilde{\theta}_N$ in Fig. b.

Clearly the largest value of $\tilde{\Gamma}_{max}$ is obtained in the case of complete even-odd staggering, which using our previous considerations amounts to very strong nuclear refraction, or a genuine physical process e.g. elastic transfer. On the other hand the minimum value of $\tilde{\Gamma}_{max}$ (~ 1.3) is attained under conditions of forward glory i.e. $\tilde{\theta}_N = -\tilde{\theta}_c$. The full curve

$\tilde{\Gamma}_{max}(-\tilde{\theta}_N)$ is symmetrical about this point. The dashed portion of this curve corresponds to positive values of $\tilde{\theta}_N$ namely short-range repulsion.

The above discussion clearly shows that an unambiguous determination of $\tilde{\Gamma}$ from the 180^{o} excitation function without explicitly considering the refraction effect of the window-like anomalous deviations, doubtful. Of course our findings are based on the Ericson parametrization. However, little qualitative change occur if other types of parametrizations are used, as we have verified with the GP.

A second point which is worth commenting upon as a consequence of the results of sec. 2 is the association of the strengths $d(E)$ and $d'(E)$ with the $\frac{\sigma}{\sigma_R}(180^{o},E)$ data. Such an association is made in refs. 4) and 5). In these papers a semiclassical multi-step α-transfer model was used to estimate the quantities $d(E)$ and $d'(E)$ in the collision $^{16}O - ^{28}Si$. These functions turned out to have[4] window-like behaviour in E-space with a maximum at $E_0 \sim 25$ MeV and exponential fall off at higher energies. It was shown later[5] that with a more realistic choice of the impact parameters involved in the semi-classical model the maximum of $d'(E)$ was shifted to $E_0' \sim 32$ MeV. The functions $d(E)$ and $d'(E)$ of ref. 5) were then directly compared to the $\frac{\sigma}{\sigma_R}(180^{o},E)$ data, as a test of the model used. Our study of the interference factors shows, however, that a direct comparison of this kind may be inappropriate. The factor $g(E)$ (eq. (2.5)) should not affect significantly the gross structure of the excitation function but taking $|d(E)|^{2}$ will make $\frac{\sigma}{\sigma_R}$ sharper in E-space and the presence of the interference factor may turn the excitation function rather different from the corresponding strengths $d(E)$ and $d'(E)$,

especially if the anomalous S-matrix is broad in ℓ-space. To investigate this point we calculated $\frac{\sigma}{\sigma_R}$ with the d(E) and d'(E) of ref. 5) using DEP for $\omega(\ell-\tilde{\ell})$ with different widths. Only Coulomb refraction was considered. The results are shown in fig. 9, together with d(E) and d'(E). The comparison between the energy E_m (E'_m) where $\frac{\sigma}{\sigma_R}$ ($\frac{\sigma'}{\sigma_R}$) has a maximum with E_0 (E'_0) shows that E_m is slightly shifted to a lower value while E'_m has a more significant shift towards higher energies, specially for broad $\omega(\ell-\tilde{\ell})$. The difference between the half-width of the strength d(E) (d'(E)) and that of $\frac{\sigma}{\sigma_R}$ is of the order of 1 MeV. In fig. 10 we show that the excitation functions obtained with the DEP can be put in agreement with the gross structure of the data if a rather broad ($\tilde{\Gamma} \simeq 5$) $\omega'(\ell-\tilde{\ell})$ is used. This of course, is clear from fig. 8b.

4. CONCLUSIONS

We have studied interference effects in the partial wave series for the scattering amplitude associated with anomalous deviations of the S-matrix, having the shape of windows in ℓ-space. Through the introduction of an interference factor a(E) we stablished a criterion to define whether the overall effect of the interference is constructive or destructive. This criterion was then applied to the anomalous scattering produced in different situations. Firstly we have determined no-refraction limits for a(E) and a'(E), which give, respectively, the strongest cancellation possible and the maximum coherence. We have then studied the effects of introducing Coulomb and nuclear phase-shifts. The introduction of Coulomb phases

was shown to lead to rather different interference factors. Although a(E) and a'(E) approach their no-refraction limits as $E \to \infty$, the situation is dramatically different at energies near the potential barrier E_B, where the tendencies of the factors a(E) and a'(E) are interchanged. It happens in this case that the introduction of a parity dependence in the anomalous S-matrix produces strong cancellation in the back-angle excitation function. The main effect of considering nuclear phase-shifts is that the interference factors approach no-refraction limits at a finite energy for which the partial wave $\tilde{\ell}(E)$ produces forward glory. The influence of shapes and half-widths of the functions $\omega(\ell-\tilde{\ell})$ which describe the anomalous S-matrix on the interference factors was studied. The main conclusions about these points is that the speed with which a(E) and a'(E) change with energy grows as $\tilde{\Gamma}$ increases and that a(E) shows oscillations with the "natural" period of eq. (2.28) for small values of $\tilde{\Gamma}$ ($\tilde{\Gamma} \lesssim 1$) or very high energies ($E >> 40$ MeV). The effects of asymmetry in $\omega(\ell-\tilde{\ell})$ were also considered. We have found that it produces oscillations in a(E) with the same "natural" period and leads to a weaker high energy fall off in this factor. Approximate analytical expressions for a(E) and a'(E) based upon the Poisson series, along the lines of ref. 8), were derived in all cases mentioned above and were shown to be in good agreement with the numerical summation of the partial waves series.

In light of the properties of a(E) and a'(E) some considerations about the study[2,3] of the anomalous excitation functions of $^{16}O + ^{28}Si$ were made. Our main conclusion is that an unambiguous determination of the half-width $\tilde{\Gamma}$ from the 180°-excitation function without due considerations of the nuclear

refraction effects attached to the underlying anomalous deviations, is doubtful. We have shown also that a(E) or a'(E) way play a very important role in the energy dependence of $\sigma(E,180^{o})$ and that a direct comparison between the strengths d(E) or d'(E) and the ratio $\frac{\sigma}{\sigma_R}$ may be misleading.

ACKNOWLEDGEMENTS

Fruitful discussions with Dr. Raul Donangelo during the preliminary stages of this work are aknowledged.

REFERENCES

1) P. Braun-Munzinger and J. Barrette, Phys. Rep. C87 (1982) 209.

2) W.E. Frahn, M.S. Hussein, L.F. Canto and R. Donangelo, Nucl. Phys. A369 (1981) 166.

3) M.S. Hussein and M.P. Pato, Phys. Rev. C25 (1982) 1896.

4) L.F. Canto, R. Donangelo, M.S. Hussein and A. Lepine-Szily, Phys. Rev. Lett. 51 (1983) 95.

5) M.S. Hussein, L.F. Canto and R. Donangelo, Phys. Rev. C29 (1984) 2383.

6) T.E.O. Ericson, in Preludes in Theoretical Physics, Ed. A. De-Shalit, H. Feshbach and L. van Hove (North-Holland, Amsterdam, 1965) p. 301.

7) W.E. Frahn, Nucl. Phys. A337 (1980) 324.

8) Abramowitz and Stegun, in "Handbook of Mathematical Functions", Ed. Dover Publ., Inc., New York, 1970.

9) P. Braun-Munzinger et al., Brookhaven National Laboratory Report Nº 28405; Phys. Rev. C24 (1981) 1010.

FIGURE CAPTIONS

FIG. 1 - Exact (full lines) and approximate (crosses) interference factors in the DEP including Coulomb refraction. No refraction limits are indicated by dashed lines (for $\tilde{\Gamma} = 3$ C lies below 10^{-7}). For details see the text.

FIG. 2 - Exact (full lines) and approximate (crosses) interference factors in the GP, including Coulomb refraction. No refraction limits are indicated by dashed lines (for $\tilde{\Gamma} = 3$ C lies below 10^{-16}). For details see the text.

FIG. 3 - Study of cancellations in the partial waves summation (eq. (2.7)), for $\tilde{S}$ in the form of eq. (2.9).

FIG. 4 - Interference factors with the DEP, including Coulomb plus nuclear refraction. Figures a, b, c, d and e correspond, respectively, to $\tilde{\theta}_N = 0, -.25\pi, -0.50\pi, -.75\pi$ and $-\pi$.

FIG. 5 - Interference factor a(E) for asymmetric shape functions. Full lines correspond to the parametrization of eq. (2.15) with $\tilde{\Gamma}_1 = 1.5$, $\tilde{\Gamma}_2 = 2.0$ and with $\tilde{\Gamma}_1 = 2.0$, $\tilde{\Gamma}_2 = 1.5$. Results for symmetric GP with $\Gamma = 1.5$ and $\Gamma = 2.0$ are also shown (crosses).

FIG. 6 - Interference factor a'(E). The details are the same as Fig. 5.

FIG. 7 - Interference factors for asymmetric shape functions. Full lines correspond to exact partial-waves summation (eq. (2.7)). Dotted lines correspond to approximate analytic expressions with the leading term $m = -1$. For details see the text.

FIG. 8 - Connection between d(E) and $\tilde{\Gamma}$ compatible with the data and the unitarity constraint of $\tilde{S}$ (see text for details). The numbers attached to the curves in Fig. 8a correspond to the values of $\tilde{\theta}_N$ in units of π.

FIG. 9 - Excitation function for $^{16}O - ^{28}Si$ elastic scattering at 180°, calculated with the strengths of ref. 5) (indicated by dots) and DEP with $\tilde{\Gamma} = 2$ and $\tilde{\Gamma}' = 5$.

FIG. 10 - Excitation function for $^{16}O - ^{28}Si$ elastic scattering at 180°. Full lines are calculations with DEP with $\tilde{\Gamma} = 1.4$ and $\tilde{\Gamma}' = 5.0$ and the strengths of ref. 5). Crosses are experimental points from ref. 9).

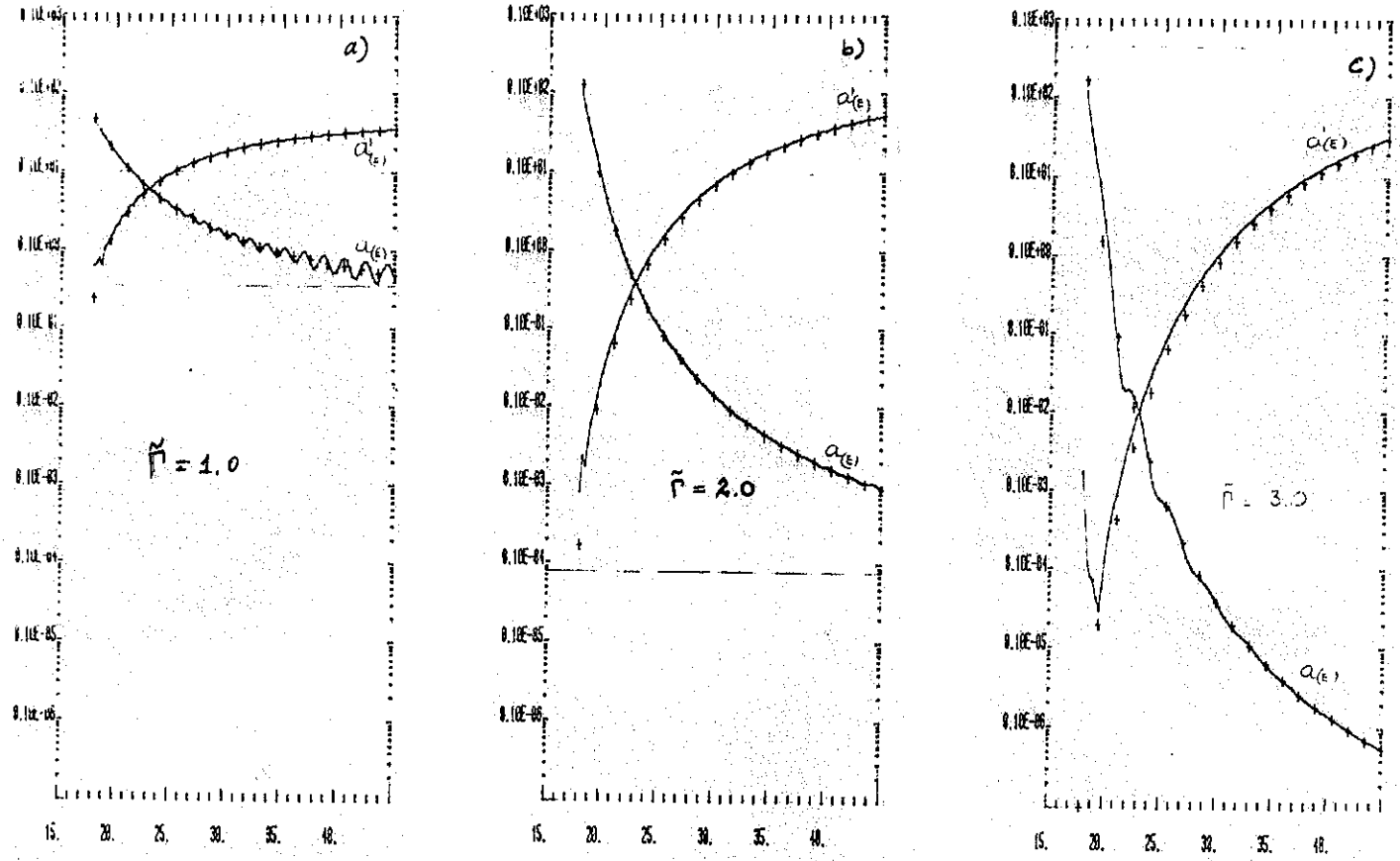
a)
b)
c)
$\tilde{\Gamma} = 1.0$
$\tilde{\Gamma} = 2.0$
$\tilde{\Gamma} = 3.0$
$a'_{(\varepsilon)}$
$a_{(\varepsilon)}$
15. 20. 25. 30. 35. 40.

FIG. 1

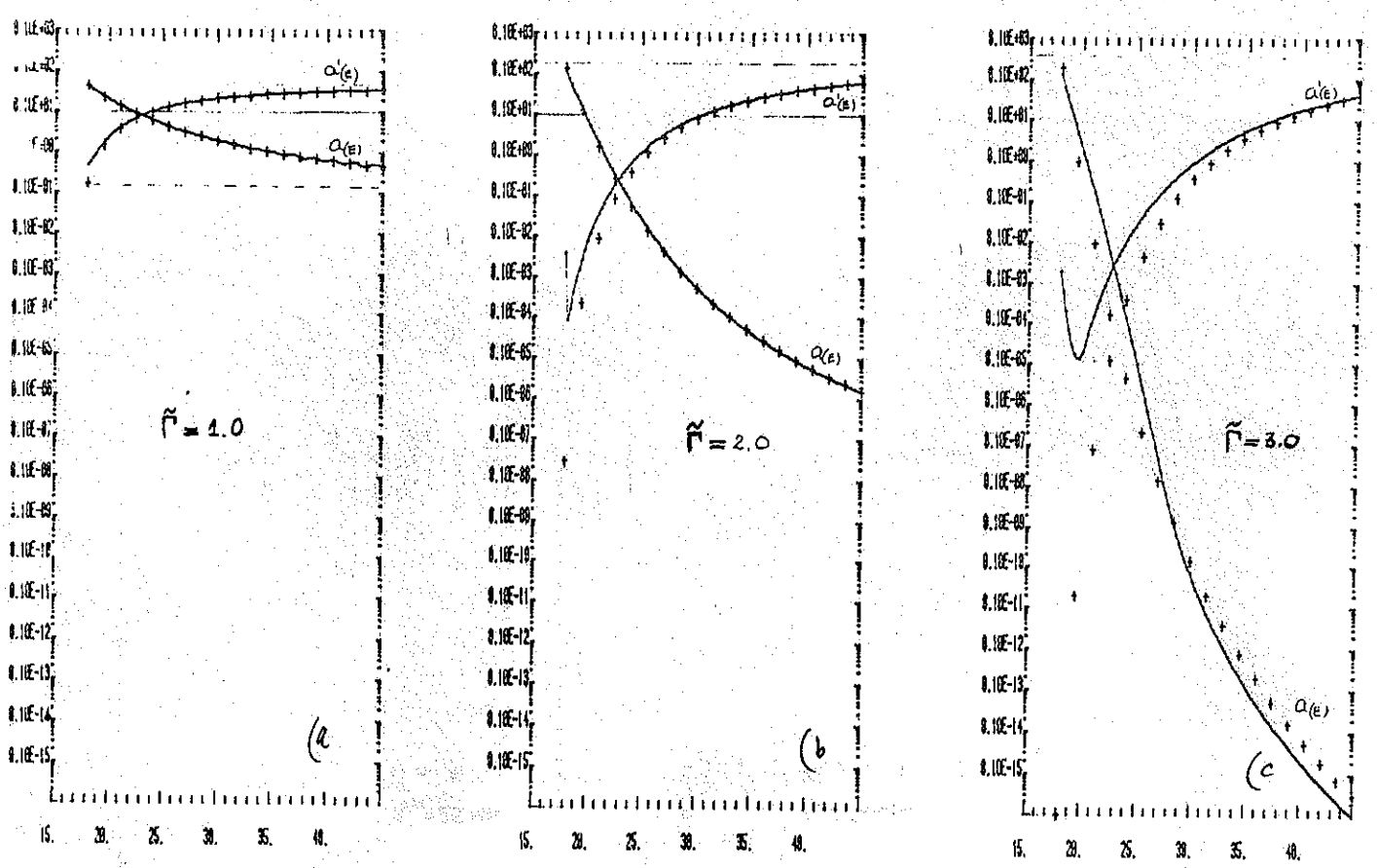
(a)
(b)
(c)
$\tilde{\Gamma} = 1.0$
$\tilde{\Gamma} = 2.0$
$\tilde{\Gamma} = 3.0$
$a'_{(\varepsilon)}$
$a_{(\varepsilon)}$
15. 20. 25. 30. 35. 40.

FIG. 2

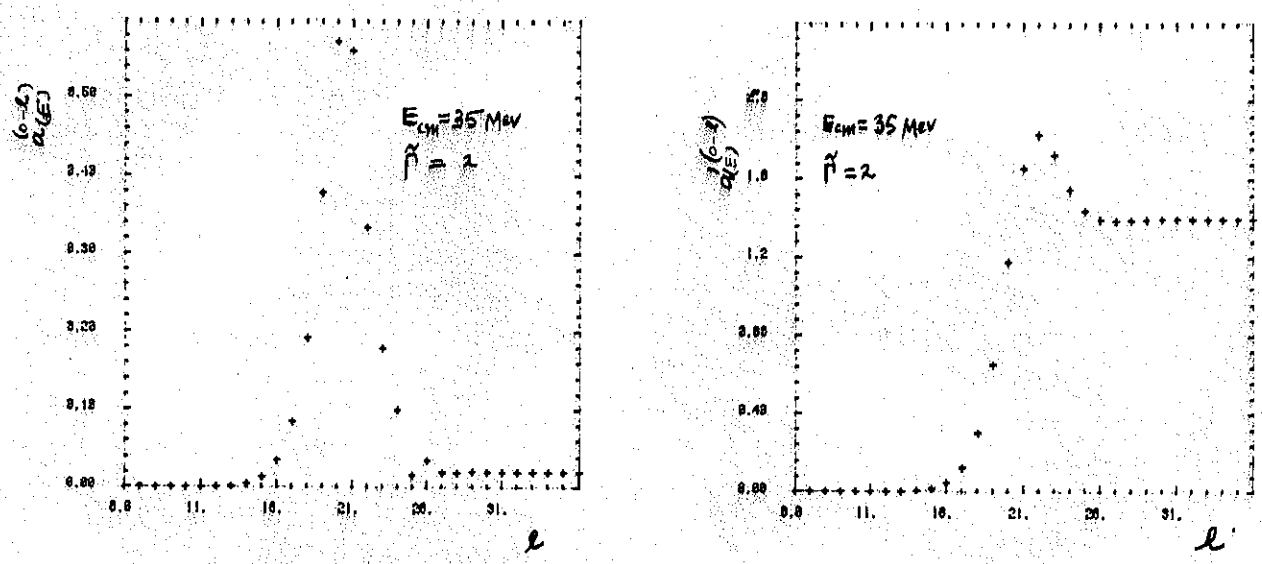

FIG. 3

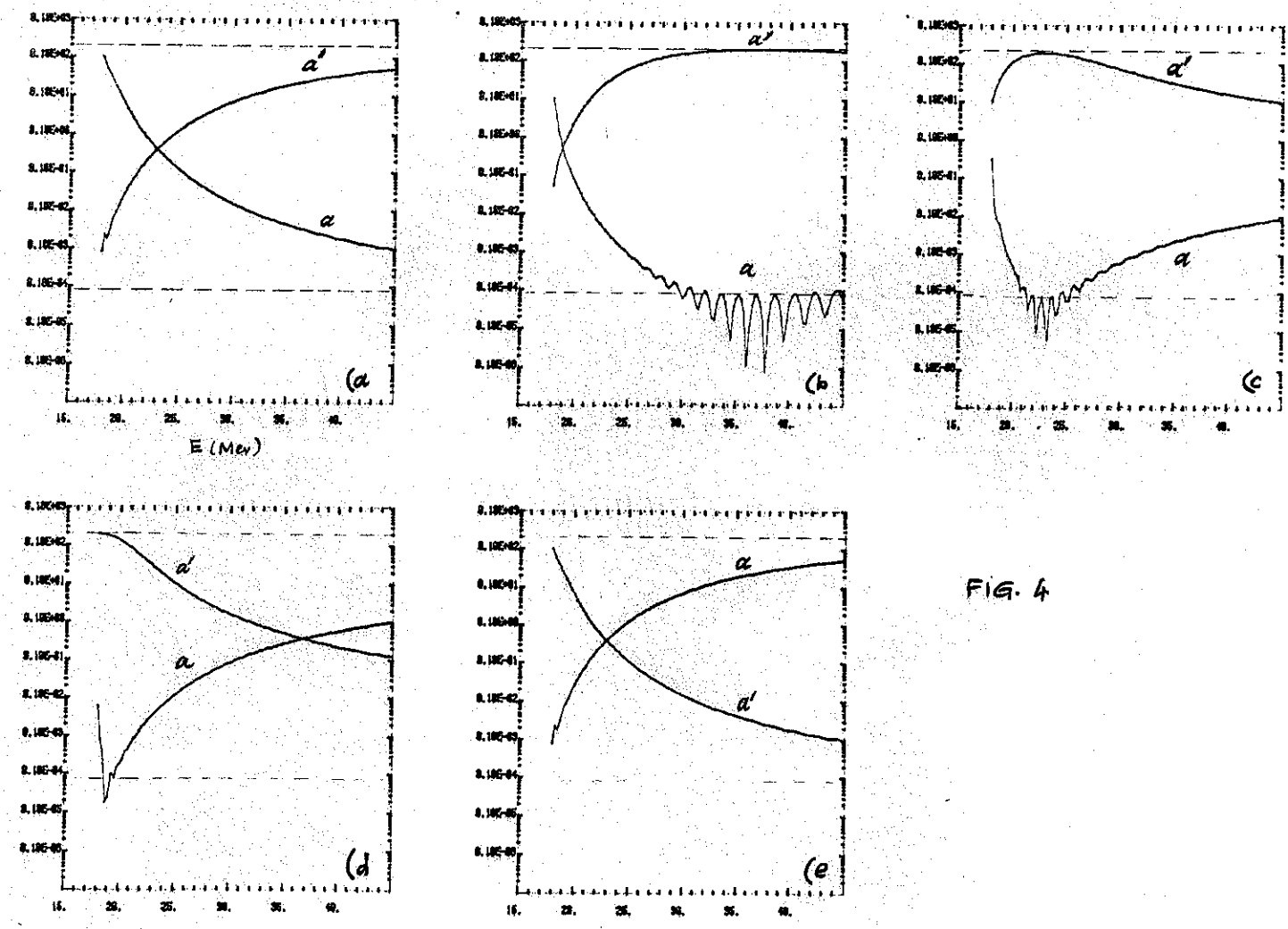

FIG. 4

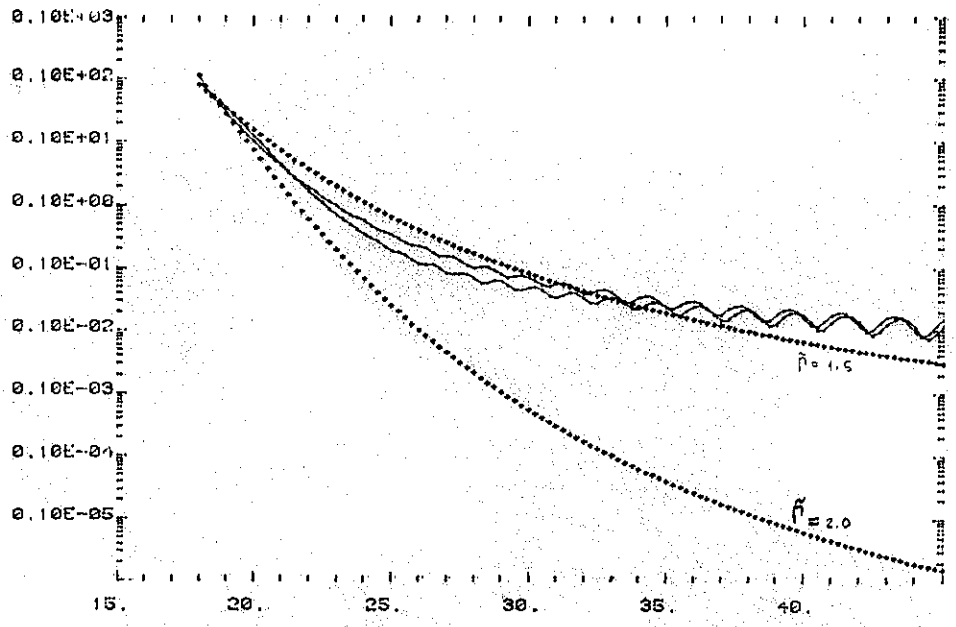
0.10E+03
0.10E+02
0.10E+01
0.10E+00
0.10E-01
0.10E-02
0.10E-03
0.10E-04
0.10E-05
15.
20.
25.
30.
35.
40.
$\tilde{\rho}=1.5$
$\tilde{\rho}=2.0$

Fig.5

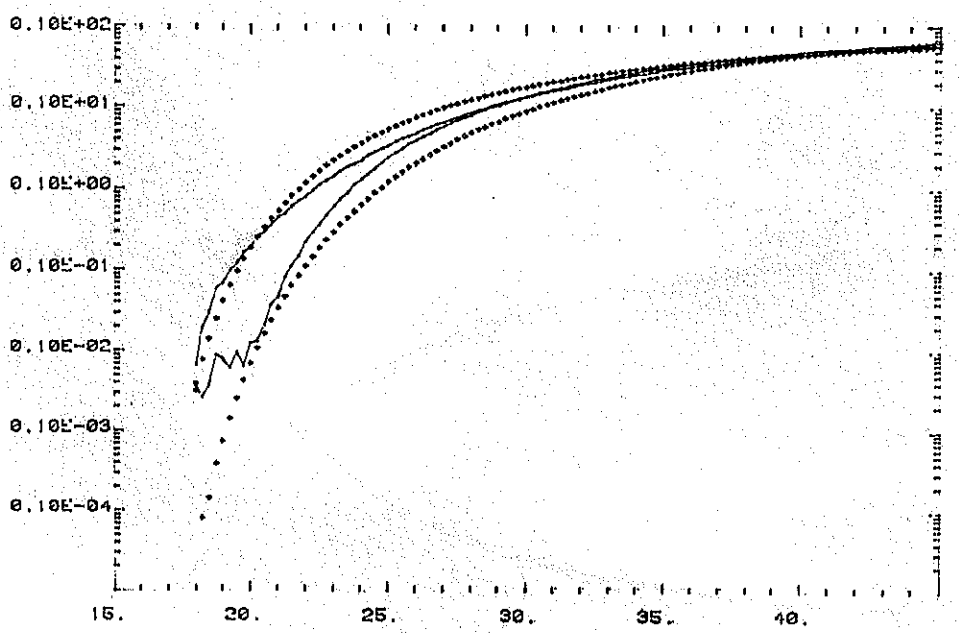
0.10E+02
0.10E+01
0.10E+00
0.10E-01
0.10E-02
0.10E-03
0.10E-04
15.
20.
25.
30.
35.
40.

Fig.6

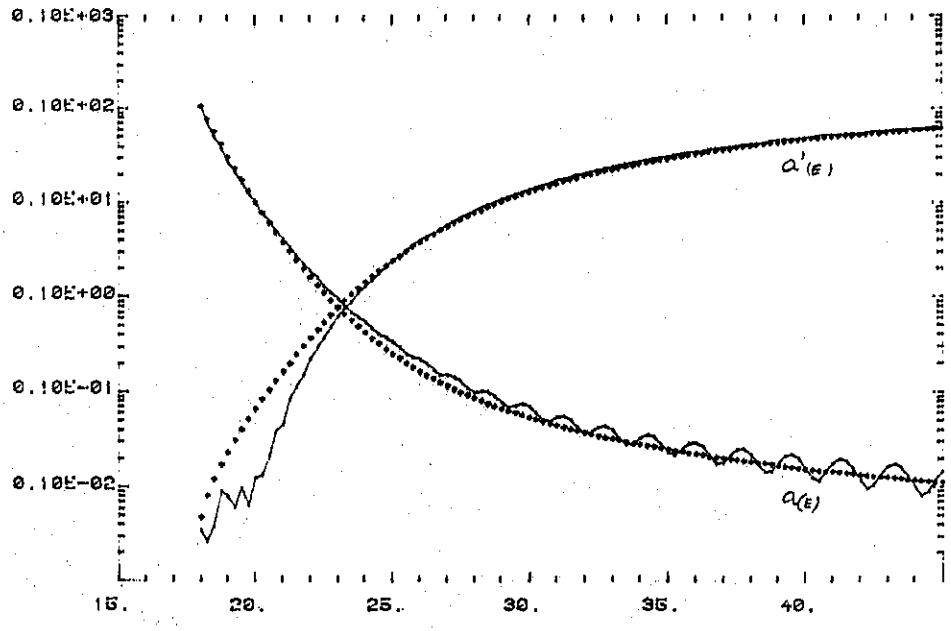
0.10E+03
0.10E+02
0.10E+01
0.10E+00
0.10E-01
0.10E-02
15.
20.
25.
30.
35.
40.
a'(E)
a(E)

Fig. 7

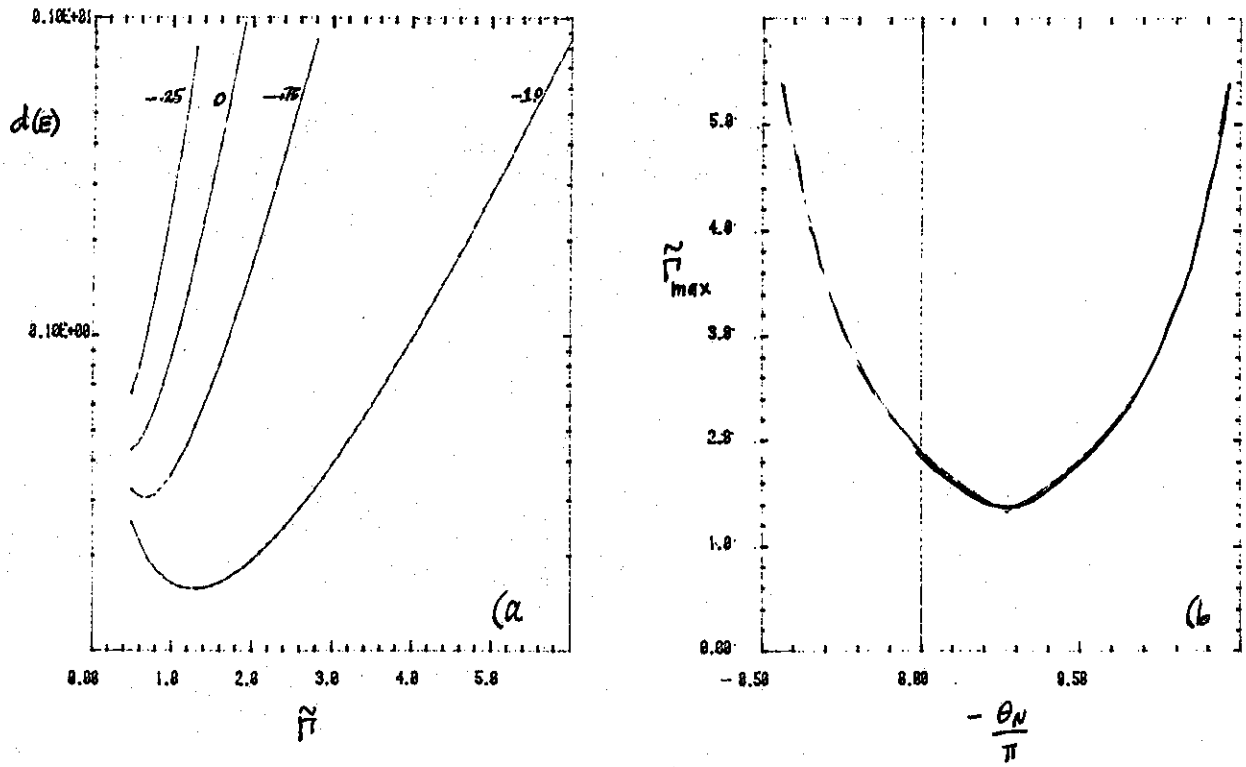
d(E)
-.25
0
-.75
-1.0
(a
0.00
1.0
2.0
3.0
4.0
5.0
Γ̃
Γ̃max
5.0
4.0
3.0
2.0
1.0
0.00
-0.50
0.00
0.50
(b
-θN/π

FIG. 8

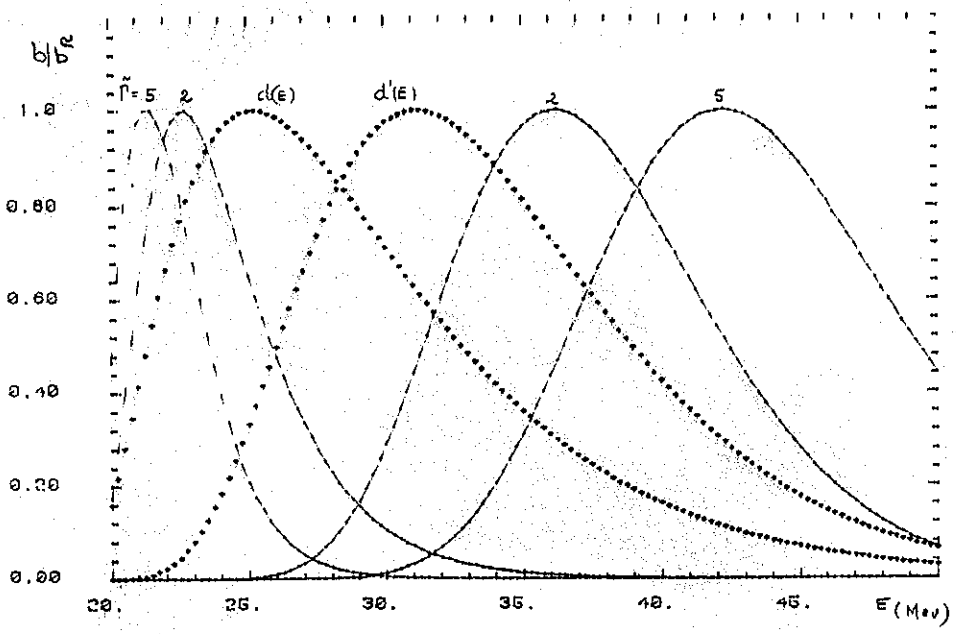
σ/σR
Γ̃= 5
2
d(E)
d'(E)
2
5
1.0
0.80
0.60
0.40
0.20
0.00
20.
25.
30.
35.
40.
45.
E(MeV)

FIG. 9

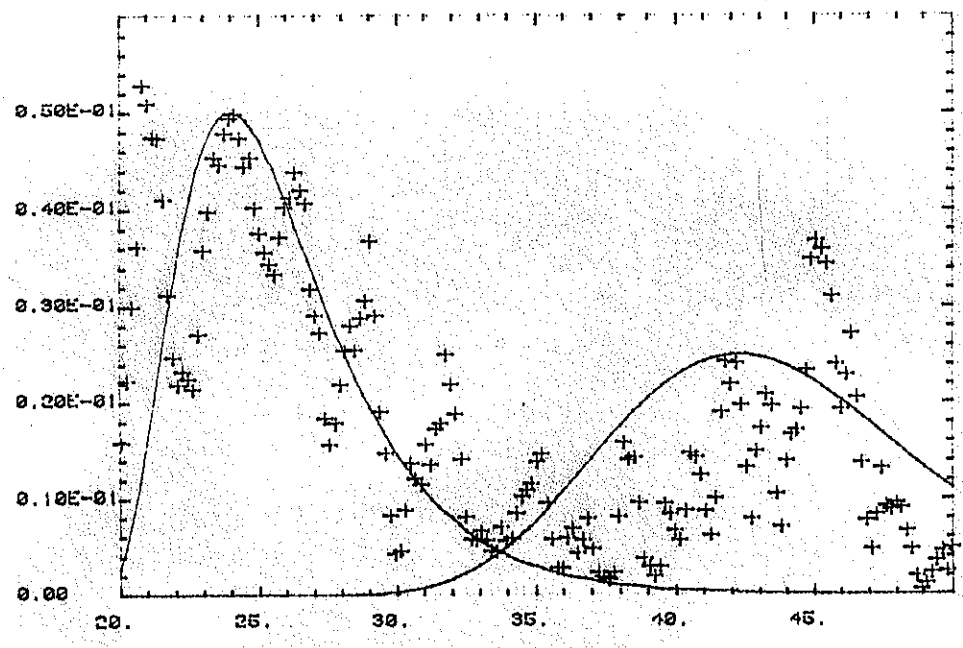
0.50E-01
0.40E-01
0.30E-01
0.20E-01
0.10E-01
0.00
20.
25.
30.
35.
40.
45.

FIG. 10